Polymorphism of LaTaTiO$_6$

Marta Kasunič,[1]* Srečo D. Škapin,[2] Danilo Suvorov[2] and Amalija Golobič[1]

[1] *Faculty of Chemistry and Chemical Technology, University of Ljubljana, Aškerčeva 5, 1000 Ljubljana, Slovenia*

[2] *Jožef Stefan Institute, Jamova 39, 1000 Ljubljana, Slovenia*

* *Corresponding author: E-mail: marta.kasunic @fkkt.uni-lj.si*

Abstract

Two polymorphs of LaTaTiO$_6$, i.e. monoclinic and orthorhombic, were synthesized by solid-state reaction technique. Both were found to be isostructural with analogous niobium compounds which were used as structural models. Structural characterization was performed on X-ray powder data by Rietveld refinement procedure which resulted in final R_{wp} values of 7.01 and 7.52% for orthorhombic and monoclinic form, respectively. Comparisons between both title compounds are given and their plausibility is proved by bond valence sums and global instability index calculations. For the monoclinic polymorph, dielectric properties measured at 1 MHz are also given.

Keywords: X-ray powder diffraction, crystal structure, polymorphism, ternary system La$_2$O$_3$-TiO$_2$-Ta$_2$O$_5$, LaTaTiO$_6$.

1. Introduction

Different lanthanum titanates are known for their pronounced dielectric properties that are of interest mainly in wireless communications applications.[1,2] Plenty of them have been prepared while trying to stabilize the unstable perovskite La$_{2/3}$TiO$_3$ compound with the addition of the third metal oxide into the La$_2$O$_3$–TiO$_2$ system.[3,1] With this aim, the following metal oxides were used: MgO,[4] CaO,[5–7] SrO,[7–9] BaO amongst earth-alkali metals,[7] Al$_2$O$_3$ and Ga$_2$O$_3$ of group III elements,[10–13] SiO$_2$,[14] GeO$_2$ and PbO of group IV,[15,16] Mn$_2$O$_3$ and Fe$_2$O$_3$ of the first row transition elements,[17,18] ZrO$_2$ and Nb$_2$O$_5$ of second row transition elements.[19–21] All these ternary systems and their thermal equilibria were widely studied and the effort resulted in a formation of numerous new compounds.

However, little is known about the equilibria and crystal structures in ternary system with Ta$_2$O$_5$. To the best of our knowledge, until now, few ternary oxides were prepared, but only one crystal structure has been determined (La$_3$Ti$_2$TaO$_{11}$) while several others have been proposed to be representatives of slab perovskite-like structures.[22,23] The motivation to explore this system were similarities between ionic radii and other chemical features of Ta^{5+} and Nb^{5+} that should enable preparation of new (possibly isostructural) compounds. Recently, the structural features

of orthorhombic LaTaTiO$_6$ were published as a part of a *Ln*TaTiO$_6$ series (*Ln* = trivalent lanthanoid) with the characteristic structural change from aeschynite to euxenite type as a consequence of different *Ln*$^{3+}$ ionic radii.[25] Herein, we report on the synthesis and structures of two LaTaTiO$_6$ polymorphs and their interconversion as a consequence of the synthesis temperature change. The plausibility of both crystal structures was additionally confirmed by bond valence sums and global instability index calculations. For the monoclinic form, the dielectric properties are also given.

2. Experimental

2. 1. Materials and Synthesis

Both polymorphs of LaTaTiO$_6$ were prepared as pale yellow powders by the conventional solid-state reaction technique, using La$_2$O$_3$ (Alfa Aesar 99.99%), Ta$_2$O$_5$ (Alfa Aesar 99.85%) and TiO$_2$ (Alfa Aesar 99.8%). Prior to weighing the weight loss of La$_2$O$_3$ was checked by heating at 1300 °C.

Stoichiometric amounts of oxides were homogenized in a mortar and then milled in a YTZ planetary ball mill using ethanol as a media. Dried powders were uniaxially pressed into pellets and calcined in air at 1100 °C for 20 h. After the first calcination the powders were crus-

hed and milled in a planetary mill, dried, pressed and sintered at temperatures from 1100 to 1420 °C for 20 h, in order to obtain orthorhombic and monoclinic polymorphs, respectively. The samples were quenched in air afterwards.

2. 2. Physical Measurements

The capacitance and dielectric losses were measured at 1 MHz using Agilent 4284A LCR meter in temperature range from 20 to 90 °C. Due to the porosity of the orthorhombic polymorph which was already observed in literature the measurements were performed only for the monoclinic form.[25] For the same reason, the polished and thermally etched cross-sections were analyzed only for the monoclinic form by using FE-SEM SUPRA 35VP (Carl Zeiss), equipped with an energy-dispersive spectrometer (EDXS, Inca 400, Oxford Instruments) and the results of elemental analysis yield molar ratio La:Ta:Ti 1:1:1. The corresponding SEM/BSI micrograph confirming the purity of the monoclinic form is shown in Fig. 1. In case of orthorhombic compound, the absence of impurity lines confirms that the composition of the product is the same as the composition of the initial reaction mixture.

Powder X-ray diffraction data for the structural characterization were collected on Panalytical X'Pert PRO MPD powder diffractometer equipped with Ge(111) Jo-
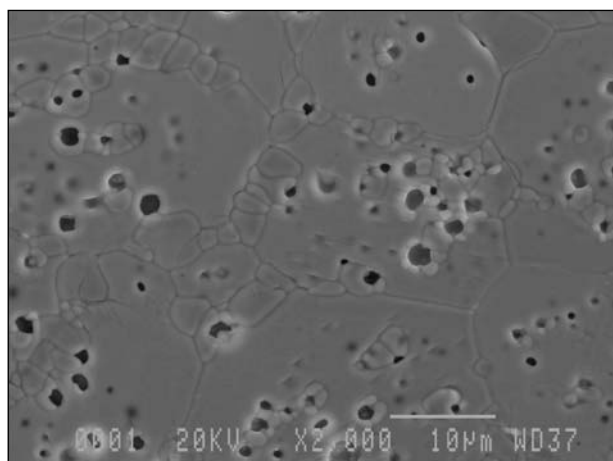
Figure 1: SEI/BSI micrograph of polished and thermally etched cross-section of the ceramic based on the compound $LaTiTaO_6$, sintered at 1420 °C for 20 h (i.e. monoclinic polymorph).

hannson type monochromator. For Rietveld refinement, Topas Academic program suite was used.[24] An initial extensive PDF-database search showed resemblance of experimental powder patterns with these of $LaNbTiO_6$.[26,27] Therefore, coordinates of both orthorhombic and monoclinic forms of $LaNbTiO_6$ were used as starting models. During the Rietveld refinement procedure, in both cases the background was described with a third order Cheby-

Table 1: Crystal data, data collection and refinement data.

Crystal data		
Chemical formula	LaO_6TaTi	LaO_6TaTi
M_r	463.73	463.73
Crystal system, space group	Monoclinic, *C2/c*	Orthorhombic, *Pnma*
Temperature of measurement (K)	293	293
a, b, c (Å)	11.23779(7), 8.86188(6), 5.27180(3)	10.94020(7), 7.57994(4), 5.45951(3)
β (°)	115.3982(4)	90
V (Å^3)	474.265(6)	452.736(5)
Z	4	4
Radiation type	Cu Ka_1, $\lambda = 1.54059$ Å	Cu Ka_1, $\lambda = 1.54059$ Å
μ (mm^{-1})	33.445	35.036
Specimen form, colour	Irregular, pale yellow powder	Irregular, pale yellow powder
Data collection		
Diffractometer	PANalytical X'Pert PRO MPD diffractometer	PANalytical X'Pert PRO MPD diffractometer
Specimen mounting	Flat plate	Flat plate
Data collection mode	Reflection	Reflection
Scan method	Continuous	Continuous
2θ values (°)	$2\theta_{min} = 10$, $2\theta_{max} = 120$, $2\theta_{step} = 0.033$	$2\theta_{min} = 12$, $2\theta_{max} = 120$, $2\theta_{step} = 0.033$
Refinement		
R factors and goodness of fit	$R_p = 0.059$, $R_{wp} = 0.075$, $R_{exp} = 0.034$, $R_{Bragg} = 0.042$, $\chi^2 = 2.236$	$R_p = 0.054$, $R_{wp} = 0.070$, $R_{exp} = 0.031$, $R_{Bragg} = 0.017$, $\chi^2 = 2.243$
Excluded regions	none	none
No. of data points	3333	3273
No. of parameters	33	33
No. of restraints	0	0

shev polynomial and for the description of peak profiles, Thompson-Cox-Hastings pseudo-Voigt function was used.[28] The scale factor, zero error, unit cell parameters together with atomic positions were also refined. In case of monoclinic polymorph, one isotropic displacement parameter for all atoms was refined and in case of orthorhombic phase, three of them were included into refinement, each for a specific atom type. Altogether 33 parameters were refined for each polymorph. The refinement proceeded smoothly and resulted in R_{wp} values of 7.01% and 7.52% for orthorhombic and monoclinic phase, respectively. Rietveld plots for 2theta range 10(12)–60 degrees can be seen in Figure 2 (for the whole 2theta range, they can be found in Supporting Information). Details on data collection and refinement as well as crystal data are given in Table 1.
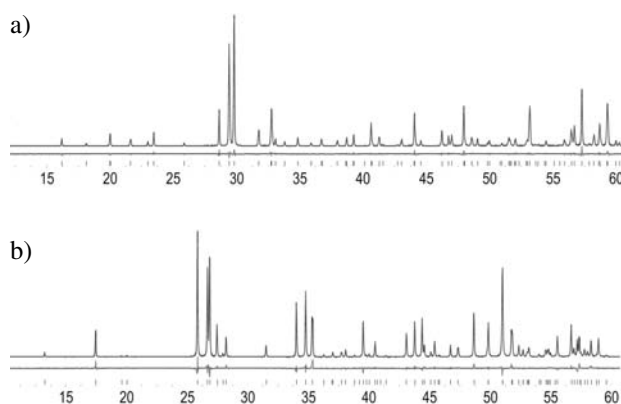
Figure 2: Rietveld plots for (a) orthorhombic and (b) monoclinic polymorph for 2theta range 10(12)–60° (experimental=blue, calculated=red, difference profile=grey). Lower vertical bars represent reflection positions. Intensity in arbitrary units.

3. Results and Discussion

3. 1. Description of Structures of Both Polymorphs

The fundamental building unit of both title compounds is BO_6 octahedron (B=Ta, Ti) in which site B is statistically occupied by tantalum and titanium ions. Negatively charged BO_6 octahedral network is charge-balanced with lanthanum cations. Common formula for both compounds is AB_2O_6.

Crystal data for both polymorphs and their atomic coordinates together with site occupancies and isotropic displacement parameters are presented in Tables 1 and 2, respectively.

The **orthorhombic** polymorph represents a structure of aeschynite type which seems to be quite frequent in the group of tantalum compounds with large cations, e.g. $EuTa_2O_6$,[29] $SrTa_2O_6$[30] and $CaTa_2O_6$.[31] Some compounds in which Ta (or Nb cations) are partially exchanged with Ti^{4+} of similar size and/or mixed occupation of large cations' sites also crystallize in this structure type, e.g. $CeNbTiO_6$[32] and $LaNbTiO_6$[26] amongst ternary oxides and stoichiometrically more complex $(Ca_{0.75}Ce_{0.25})(Nb_{0.95}Ta_{0.63}Ti_{0.42})O_6$.[33] For the aforementioned oxides, only in the case of $LaNbTiO_6$, polymorphism between orthorhombic and monoclinic polymorph was observed,[26, 27] and for the case of $CaTa_2O_6$ an orthorhombic and cubic (i. e. A-deficient perovskite) polymorphs were described.[31,34]

In the aeschynite structure type pairs of edge-sharing octahedra (($(Ta,Ti)_2O_{10}$-units) connect *via* axial oxygens O3 and O4 (both lying on a mirror plane, Wyckof site 4*c*) into double octahedral chains. These are further connected with four adjacent double chains of the same

Table 2: Atomic coordinates, occupancies and isotropic displacement parameters for both LaTaTiO₆ polymorphs.

	x	y	z	*Occ.*	B_{iso}
Monoclinic polymorph					
La1	0.5	0.6974(1)	0.25	1	0.24(2)
Ta1	0.2653(1)	0.9179(1)	–0.4502(2)	0.5	0.24(2)
Ti1	0.2653(1)	0.9179(1)	–0.4502(2)	0.5	0.24(2)
O1	0.3563(7)	0.917(1)	–0.044(2)	1	0.24(2)
O2	0.6447(8)	0.7525(9)	0.037(2)	1	0.24(2)
O3	0.6433(8)	0.545(1)	0.652(2)	1	0.24(2)
Orthorhombic polymorph					
La1	0.04176(9)	0.25	0.5411(2)	1	0.53(2)
Ta1	0.14358(8)	–0.0050(1)	0.0398(2)	0.5	0.35(2)
Ti1	0.14358(8)	–0.0050(1)	0.0398(2)	0.5	0.35(2)
O1	–0.0233(7)	0.0344(9)	0.227(1)	1	0.21(9)
O2	0.2128(7)	0.0547(9)	0.369(1)	1	0.21(9)
O3	0.1447(9)	0.25	–0.042(2)	1	0.21(9)
O4	0.1255(9)	–0.25	0.146(2)	1	0.21(9)

kind *via* (yet unshared) four equatorial vertices and negatively charged $(TaTiO_6)^{3-}$ network is thus obtained. Lanthanum counter-cations are positioned on mirror planes at Wyckoff site 4*c* forming a link between special positioned O3 and O4 oxygens from the same double chain with similar La–O(3,4) bond distances around 2.5 Å. The orthorhombic structure with characteristic aeschynite channels is depicted in Figure 3.

The distance between the octahedral cations that share an edge is 3.1725(12) Å. The distances between corner-sharing octahedral cations are 3.7135(13) and 3.8664(13) Å within the same double-octahedral chain, and 3.5887(13) Å between the adjacent ones. Lanthanum ions from the same channel are 3.9243(4) Å apart while those from different channels are of course further apart from each other, i. e. 5.9267(14) Å or more. The distance ranges metal-oxygen and coordination numbers are presented in Table 3.

As already elucidated by Jahnberg, aeschynite structure type is closely related to perovskite type.[31] The main difference is the presence of double-octahedral chains (edge and corner-sharing) in aeschynites instead of single octahedral chains in perovskites where only corner-sharing between octahedra is present.
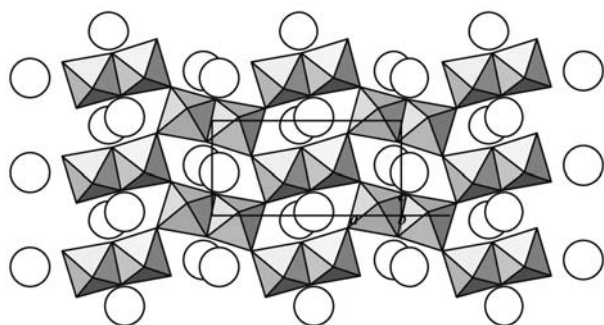
Figure 3: The polyhedral representation of the orthorhombic LaTaTiO$_6$ polymorph with characteristic double octahedral (TaTiO$_6$)-chains and intermediate La^{3+} ions.

In the **monoclinic** form only edge-sharing between BO$_6$ octahedra is present (three edges of each octahedron are shared with three adjacent octahedra). The obtained structure comprises (100) layers of corundum-like fused hexagonal rings. In this way, negatively charged (TaTiO$_6$)$^{3-}$ layers are formed between which La^{3+} counterions are placed occupying special positions on twofold axis (Wyckof site 4*e*). Each of them is coordinated with 8 oxygens, four from each of the adjacent anionic layers, in a shape of fourfold antiprism. The La–O distances in the aforementioned fourfold antiprism towards both anionic layers are the same and are in the range 2.388(10) – 2.863(10) Å. The first coordination spheres of Ta and Ti ions are presented in Table 3. The view on the monoclinic structure along *b* axis is presented in Figure 4.
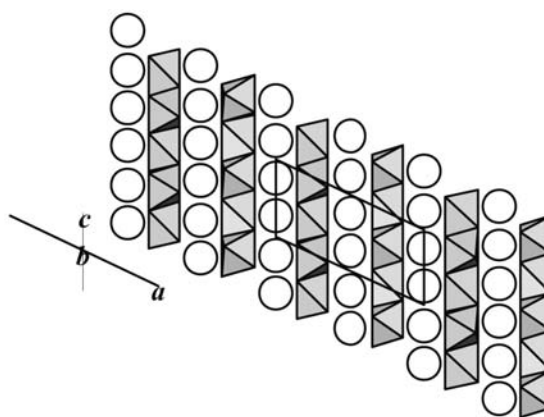
Figure 4: Representation of anionic (TaTiO$_6$)$^{3-}$ layers and intermediate La^{3+} cations in monoclinic LaTaTiO$_6$.

The monoclinic structure is related to PbSb$_2$O$_6$-structure type which consists of the same structural motif but possesses higher (trigonal) symmetry.[35] For clarity, only metal ions will be used for their comparison. In PbSb$_2$O$_6$, hexagonal rings formed by Sb^{5+} ions are completely regular and planar. Moreover, Pb^{2+} ions are positioned in the centres of these hexagonal rings and the hexagons coincide (they lie exactly one over another with no displacements). However, in LaTaTiO$_6$ hexagons formed by Ta/Ti atoms are not far from regular with four Ta/Ti–Ta/Ti distances of 3.0105(17) Å and two of 3.0164(16) Å and their internal angles are in the range between 111.53–125.91°. The maximum displacement of Ta/Ti from the described planes of Ta/Ti-defining hexagons is ±0.052(1) Å. The key difference between PbSb$_2$O$_6$ and monoclinic LaTaTiO$_6$ arises from the shifts between hexagons in bet-

a)

b)
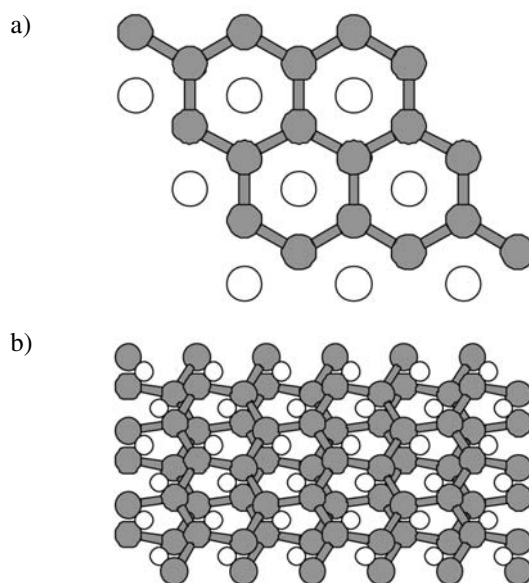
Figure 5: View on hexagonal layers formed by B-ions and A-cations in between in (a) PbSb$_2$O$_6$ and (b) monoclinic LaTaTiO$_6$.

ween adjacent layers and the shifts of La^{3+} ions from the centre of B-hexagons which lowers the symmetry to monoclinic. With these shifts A-atom changes its coordination from 12 in $PbSb_2O_6$ to 8 in $LaTaTiO_6$. The described differences are depicted in Figure 5.

The dielectric constant of the monoclinic form, measured at 1 MHz is relatively low ($\varepsilon = 25$). However, the values of electric loss ($\tan\delta = 6.7 \times 10^{-4}$) and temperature coefficient of the dielectric constant, ($\tau_k = 44$ ppm/K) which was measured between 20–90 °C, are quite low and as such promising for the use in various electronic components.

Despite of the same composition and as such, the same features of the present ions (radii, ionic charges) two completely different structures were obtained at two different synthesis temperatures. The orthorhombic phase was prepared at lower temperature as the monoclinic one (1100 vs. 1380 °C). When the pure monoclinic or pure orthorhombic phase was reheated at the intermediate temperatures and quenched in air afterwards, the reflection peaks of the other phase also appeared – the interconversion between both structures is therefore possible and reversible. In the intermediate temperature region, i.e. around 1300 °C, both phases co-exist. Powder patterns of the samples obtained at different temperatures are depicted in Figure 6.

According to Pauling, structures with more sharing of faces > edges > vertices are less stable due to larger repulsion between cations (in our case octahedrally coordinated Ta^{5+} and Ti^{4+}). When comparing metal-metal distan-

ces of both polymorphs we can conclude that edge-sharing Ta/Ti atoms in monoclinic polymorph get closer than in the orthorhombic one (3.0105(17) and 3.0164(16) Å vs. 3.1725(12) Å) and this may cause additional repulsion. The opposite is true for distances between La^{3+} ions which are shorter in the orthorhombic form where La^{3+} ions are positioned in the channels and are 3.9243(4) Å apart while in the monoclinic form La–La distances 4.3799(13) Å within the layer and 5.1658(3) Å between the layers.

3. 2. Bond Valence Sums and Global Instability Index Analysis

Bond valence sums for metal ions together with the corresponding distance ranges towards oxygen atoms, as well as global instability indices for both structures, are given in Table 3. Bond valence sums were calculated according to the formula $V_{ij} = \sum_j e^{\frac{R_0 - R_{ij}}{B}}$ where R_0 and R_{ij} are expected and experimentally determined bond lengths between the atoms i and j, and B is a constant (0.37 Å for oxide compounds). Values of R_0 as proposed by Brown & Altermatt (2.172 Å for La–O, 1.920 Å for Ta–O and 1.815 Å for Ti–O) were used in all calculations.[36]

In both compounds, bond valence sums calculations fairly reproduce the expected atomic valences of metal ions and as such additionally confirm the plausibility of the obtained structures. Slightly higher values for Ta^{5+} should be connected with the larger size of the latter in
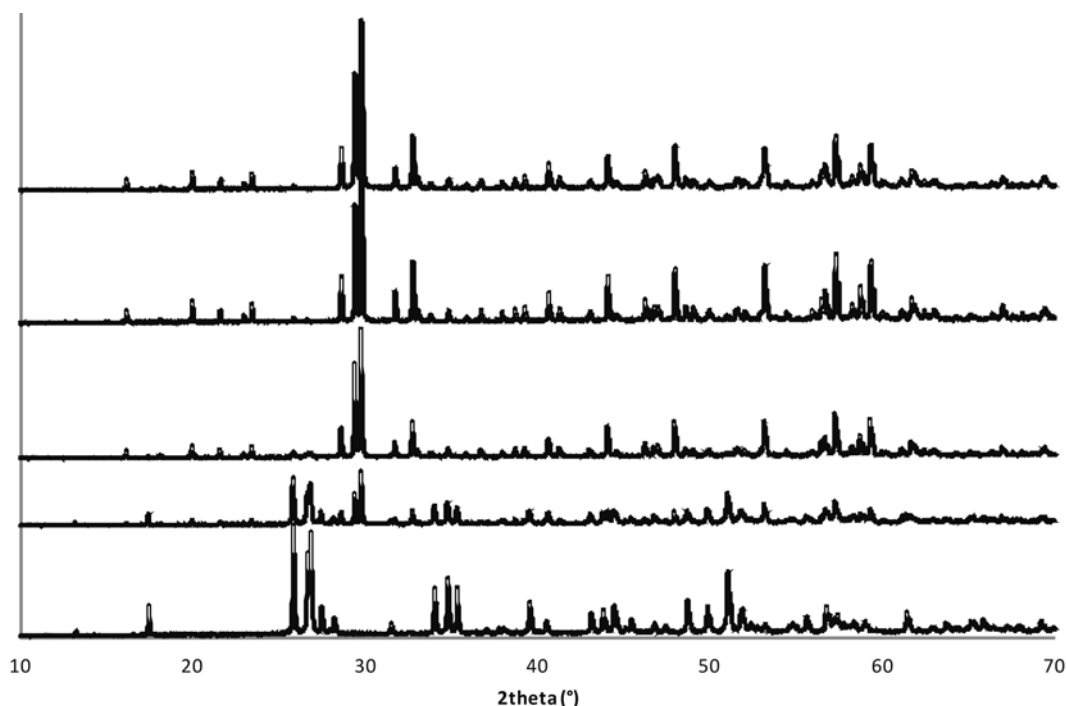
Figure 6: Powder patterns of $LaTaTiO_6$ synthesized at different temperatures, from top: 1100 (pure orthorhombic), 1200, 1300, 1350 and 1400 °C (pure monoclinic).

Table 3: Bond valence sums (BVS) together with distance ranges metal-oxygen and coordination numbers (CN) of individual ions for both LaTaTiO$_6$ polymorphs. Literature data on orthorhombic polymorph is also given for comparison. (GII = global instability index)

monoclinic LaTaTiO$_6$			
	BVS	**Distance range M – O [Å]**	**CN**
La1	3.05(3)	2.39(1) – 2.86(1)	8
Ta1	5.17(5)		6
Ti1	3.89(4)	1.939(7) – 2.02(1)	6
O1	−1.94(2)	1.939(7) – 2.578(8)	3
O2	−2.06(2)	1.945(9) – 2.39(1)	3
O3	−2.05(2)	1.979(7) – 2.86(1)	4
GII		9.34%	
orthorhombic LaTaTiO$_6$			
La1	3.17(2)	2.472(7) – 2.565(7)	8
Ta1	5.16(4)		6
Ti1	3.89(3)	1.865(8) – 2.115(8)	6
O1	−2.12(2)	1.977(7) – 2.507(7)	4
O2	−2.06(2)	1.865(8) – 2.565(7)	3
O3	−1.84(1)	1.984(3) – 2.54(1)	3
O4	−2.00(1)	1.955(3) – 2.50(1)	3
GII		12.46%	
orthorhombic LaTaTiO$_6$[25]			
La1	3.18(2)	2.471(5) – 2.563(5)	8
Ta1	5.11(2)		6
Ti1	3.85(2)	1.883(4) – 2.153(4)	6
O1	−2.10(1)	1.961(4) – 2.508(4)	4
O2	−2.05(1)	1.883(4) – 2.563(5)	3
O3	−1.847(7)	1.983(1) – 2.541(7)	3
O4	−1.988(8)	1.962(2) – 2.4917(6)	3
GII		12.25%	

comparison with Ti^{4+} as they share the same crystallographic site in the obtained (average) crystal structure.[36,37] Locally, beyond the scope of diffraction techniques, oxygen atoms probably lie somewhat closer to metal centre in TiO$_6$-octahedra and the bond lengths Ta–O are expected to be slightly longer. In both structures, BVS for La^{3+} are comparable and close to the nominal atomic valences. The same is true for the global instability index (GII) that measures the extent to which the BVS rule is violated over the whole structure.[38] Due to the similarity of individual bond valence sums, both GIIs are consequently of similar value.

Furthermore, no significant differences for the orthorhombic polymorph were observed when comparing with the literature data based on neutron and synchrotron measurements.[25] Metal-oxygen bond lengths, BVS and GII for the latter are also given in Table 3. It can be clearly seen that all aforementioned quantities do not differ much and that also in our obtained structure, oxygen positions are satisfyingly determined.

4. Conclusions

In the present paper two polymorphs of LaTaTiO$_6$ as oxides with general formula AB$_2$O$_6$, found as single pha-

ses in the ternary phase diagrams of the corresponding metal oxides, were structurally characterized. By pattern-matching it was concluded that they are isostructural with analogous niobium compounds which were used as initial structural models and refined with Rietveld refinement procedure. The orthorhombic polymorph belongs to aeschynite group while the monoclinic one reminds on trigonal PbSb$_2$O$_6$ structure. Both obtained structures comply with the rules of crystal chemistry that results in BVS not far from nominal atomic valences and low GIIs. For monoclinic polymorph, the low electric loss (tan δ = 6.7 × 10^{-4}) and temperature coefficient of the dielectric constant (τ_k = 44 ppm/K) seem to be quite promising.

The final structural data (including coordinates, displacement and geometrical parameters) have also been deposited with FIZ Karlsruhe Crystal Structure Deposition (CSD) Center as supplementary material with the deposition numbers 423393 and 423394 for monoclinic and orthorhombic LaTaTiO$_6$, respectively. Copies of the data can be obtained, free of charge, contacting crysdata@fiz-karlsruhe.de

6. References

1. S. D. Škapin, D. Kolar, D. Suvorov, *J. Eur. Ceram. Soc.* **2000**, *20*, 1179–1185.
2. H. Zhang, L. Fang, R. Elsebrock, R. Z. Yuan, *Mat. Chem. Phys.* **2005**, *93*, 450–454.
3. M. Abe, K. Uchino, *Mat. Res. Bull.* **1974**, *9*, 147–155.
4. Z. Chaogui, W. Shuangyan, L. Fuhui, T. Shujian, L. Guobao, *J. Alloys Compd.* **1999**, *289*, 257–259.
5. K. Demšar, S. D. Škapin, A. Meden, D. Suvorov, *Acta Chim. Slov.* **2008**, *55*, 966–972.
6. R. Rejini, G. Subodh, M. T. Sebastian, *J. Mater. Sci: Mater. Electron.* **2008**, *19*, 1153–1155.
7. I. N. Jawahar, N. I. Santha, M. T. Sebastian, *J. Mater. Res.* **2002**, *17*, 3084–3089.
8. H. Takamura, K. Enomoto, A. Kamegawa, M. Okada, *Solid State Ionics* **2002**, *154*, 581–588.
9. M. E. Bowden, D. A. Jefferson, I. W. M. Brown, *J. Solid State Chem.* **1995**, *119*, 412–419.
10. S. Škapin, D. Kolar, D. Suvorov, *J. Am. Ceram. Soc.* **1993**, *76*, 2359–2362.
11. D. Suvorov, M. Valant, S. Škapin, D. Kolar, *J. Mater. Science* **1998**, *33*, 85–89.
12. D. Kolar, S. Škapin, D. Suvorov, M. Valant, in: K. E. Spear (Ed.), Proceedings of the ninth international conference on

high temperature materials chemistry: Electrochemical Society Series **1997**, 97, 109–115.

13. M. Kasunič, A. Meden, S. D. Škapin, D. Suvorov, A. Golobič, *Acta Cryst.* **2009**, *B65*, 558–566.

14. M. Iwasaki, K. I. Kashimura, H. Masaki, S. Ito, *J. Sol-Gel Sci. Techn.* **2003**, *26*, 389–392.

15. M. C. Martín-Sedeño, E. R. Losilla, L. León-Reina, S. Bruque, D. Marrero-López, P. Núñez, M. A. G. Aranda, *Chem. Mater.* **2004**, *16*, 4960–4968.

16. V. V. Prisedsky, V. M. Golubitsky, *Ferroelectrics* **1992**, *131*, 283–287.

17. S. D. Škapin, Š. Kunej, D. Suvorov, *J. Eur. Ceram. Soc.* **2008**, *28*, 3119–3124.

18. S. D. Škapin, A. Sever Škapin, D. Suvorov, M. Gaberšček, *J. Eur. Ceram. Soc.* **2008**, *28*, 2025–2032.

19. S. D. Škapin, D. Kolar, D. Suvorov, *Solid State Sciences* **1999**, *1*, 245–255.

20. V. I. Strakhov, O. V. Melnikova, M. Dib, A. P. Pivovarova, O. V. Karpinskaya, *Zh. Neorg. Khim.* **1996**, *41*, 1373–1375.

21. Y. P. Udalov, V. I. Strakhov, O. V. Melnikova, O. V. Karpinskaya, M. Dib, A. P. Pivovarova, *Zh. Neorg. Khim.* **1996**, *41*, 305–308.

22. Yu. A. Titov, A. M. Sych, V. Ya. Markiv, N. M. Belyavina, A. A. Kapshuk, V. P. Yashchuk, *J. Alloys Compd.* **2001**, *316*, 309–315.

23. Yu. A. Titov, A. M. Sych, A. A. Kapshuk, V. P. Yashchuk, V. Ya. Markiv, N. M. Belyavina, *Dopov. Nats. Akad. Nauk. Ukr.* **2000**, 148–152.

24. A. A. Coelho, TOPAS-Academic, Version 4.1. Coelho Software, Brisbane, Australia.

25. G. J. Thorogood, M. Avdeev, B. J. Kennedy, *Solid State Sciences* **2010**, *12*, 1263–1269.

26. D. Fauquier, M. Gasperin, *Bulletin de la Societe Francaise de Mineralogie et de Cristallographie* **1970**, *93*, 258–259.

27. A. Golobič, S. D. Škapin, D. Suvorov, A. Meden, *Croat. Chem. Acta* **2004**, *77*, 435–446.

28. P. Thompson, D. E. Cox, J. B. Hastings, *J. Appl. Cryst.* **1987**, *20*, 79–83.

29. H. Jacobsen, F. Lissner, E. Manek, G. Meyer, *Z. Krist.* **1996**, *211*, 547–548.

30. V. P. Sirotinkin, S. P. Sirotinkin, *Zh. Neorg. Khim.* **1993**, 38, 1071–1073.

31. L. Jahnberg, *Acta Chem. Scand.* **1963**, *17*, 2548–2559.

32. V. B. Aleksandrov, *Doklady Akademii Nauk SSSR* **1962**, *142*, 181–184.

33. G. Giuseppetti, C. Tadini, *Neues Jahrbuch fuer Mineralogie. Monatshefte* **1990**, 301–308.

34. P. Tiedemann, H. Mueller Buschbaum, *Z. Anorg. Allg. Chem.* **1984**, *516*, 201–206.

35. A. Magneli, *Arkiv foer Kemi Mineralogi och Geologi* **1941**, *B15*, 1–6.

36. I. D. Brown, D. Altermatt, *Acta Cryst.* **1985**, *B41*, 244–247.

37. R. D. Shannon, *Acta Cryst.* **1976**, *A32*, 751–767.

38. A. Salinas-Sanchez, J. L. Garcia-Muñoz, J. Rodriguez-Carvajal, R. Saez-Puche, J. L. Martinez, *J. Solid State Chem.* **1992**, *100*, 201–211.

Povzetek

S pomočjo sinteze v trdnem stanju smo pripravili dve polimorfni modifikaciji LaTaTiO$_6$, monoklinsko in ortorombsko. Izkazalo se je, da sta obe izostrukturni z analognima niobijevima spojinama, ki smo ju uporabili za začetna strukturna modela. Strukturno karakterizacijo smo izvedli na osnovi rentgenskih praškovnih podatkov z Rietveldovo metodo, ki je vodila do končnih R$_{wp}$ vrednosti 7,01 % za ortorombsko oziroma 7,52 % za monoklinsko obliko. V članku so podane primerjave med kristalnima strukturama obeh polimorfov, katerih pravilnost smo dodatno potrdili z izračunom vsot veznih valenc in globalnega nestabilnostnega indeksa. Za monoklinsko obliko smo pri frekvenci 1 MHz izmerili tudi dielektrične lastnosti.